Institute of Applied Problems of Physics

Laboratory of Physics of Nano- and Mesosystems

Project 21AG-1C022

Thermodynamic and magnetic parameters of electron gas in cylindrical nanoplatelets

Hayk Sarkisyan

In collaboration with

V. Harutyunyan, Ye. Mamasakhlisov, D. Baghdasaryan, H. Ghaltakhchyan,

M. Mkrtchyan, Kh. Khachatryan L. Tadevosyan A. Nahapetyan, M. Manvelyan

T. Shahbazyan, L. Petrosyan

Dilijan 2025

Publications (2025)

Optics Communications 589 (2025) 131882

Contents lists available at ScienceDirect

Optics Communications

journal homepage: www.elsevier.com/locate/optcom

Influence of dielectric confinement and size effect on nonlinear absorption in CdSe nanoplatelets

M.K. Manvelyan [a,b], M.A. Mkrtchyan [a,b,*], Kh.S. Khachatryan [a,b], H.A. Sarkisyan [a]

[a] Institute of Applied Problems of Physics NAS RA, 25 Nersisyan St., Yerevan, 0014, Armenia

[b] Russian-Armenian University, 123 Hovsep Emin St., Yerevan, 0051, Armenia

$$V_{conf}^{(1)}(x,y) = \begin{cases} 0, & |x| \le \frac{L_1}{2}; |y| \le \frac{L_2}{2} \\ \infty, & |x| > \frac{L_1}{2}; |y| > \frac{L_2}{2} \end{cases}$$

$$V_{conf}^{(2)}(z) = \begin{cases} 0, & |z| \le \frac{L_3}{2}, \\ V_0, & |z| > \frac{L_3}{2}. \end{cases}$$

$$V_{self}(z) = \begin{cases} \sum\limits_{m=\pm1,\pm2,\dots} \frac{\kappa^{|m|} e^2}{2\varepsilon_w |z-(-1)^m z + mL_z|}, & |z| < L_z/2, \\ \frac{2\varepsilon_w}{\varepsilon_w+\varepsilon_b} \sum\limits_{m=0}^{\infty} \frac{\kappa^{2m+1} e^2}{(\varepsilon_w+\varepsilon_b)|2z+(2m+1)L_z|} - \frac{\kappa e^2}{2\varepsilon_b |2z - L_z|}, & z > L_z/2, \\ V_{self}(-z), & z < -L_z/2, \end{cases}$$

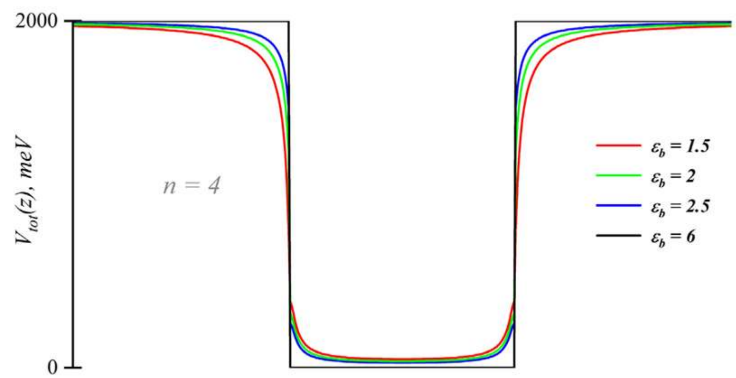

Fig. 1. $V_{tot}(z)$ dependence from $\varepsilon_b = [1.5, 2, 2.5, 6]$ for $n = 4ML$.

Publications (2025)

Nanoscale Advances

ROYAL SOCIETY OF CHEMISTRY

PAPER

View Article Online
View Journal | View Issue

Check for updates

Cite this: *Nanoscale Adv.*, 2025, **7**, 5238

Influence of an in-plane uniform electric field on 2D exciton states in CdSe nanoplatelets

Davit A. Baghdasaryan,[a] Volodya A. Harutyunyan,[a] Hayk A. Sarkisyan,[*a] Lyudvig S. Petrosyan[b] and Tigran V. Shahbazyan[b]

$$\tau_{\mathrm{rad}} = \frac{2\pi\varepsilon_0 m_0 c^3 \hbar^2}{\sqrt{\varepsilon} e^2 E_{\mathrm{exc}}^2 f}$$

$$f = \frac{E_{\mathrm{p}}}{E_{\mathrm{exc}}} \left| \int_V \psi_{\mathrm{exc}}(\vec{r}, \vec{r}) \mathrm{d}\vec{r} \right|^2$$

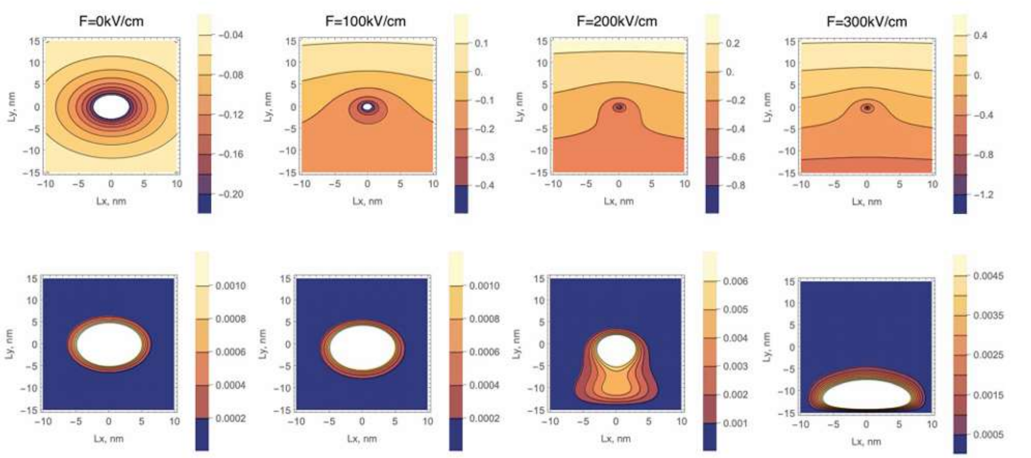

Fig. 3 The deformation of the electron–hole interaction potential under the influence of an external electric field (upper row) and redistribution of the relative motion probability density plotted in the lateral plane of NPLs (lower row) $n = 5.5$ ML. $L_x = 20$ nm and $L_y = 30$ nm.

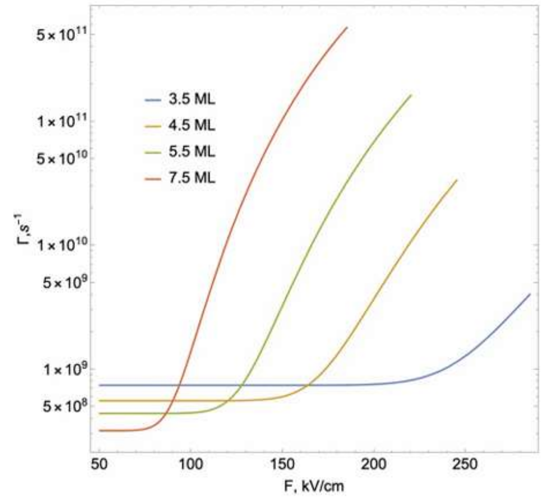

Fig. 7 Theoretical total exciton decay rate in CdSe NPLs in the presence of an external field.

Publications (2025-2026)

Journal of Physics and Chemistry of Solids 208 (2026) 113211

Contents lists available at ScienceDirect

Journal of Physics and Chemistry of Solids

journal homepage: www.elsevier.com/locate/jpcs

ELSEVIER

Diamagnetic susceptibility and binding energy of hydrogenic impurity in CdSe nanoplatelets: Effect of dielectric mismatch and size-quantization

M.K. Manvelyan [a,b], B.K. Gharibyan [c], M.A. Mkrtchyan [a,b], H.A. Sarkisyan [a,*]

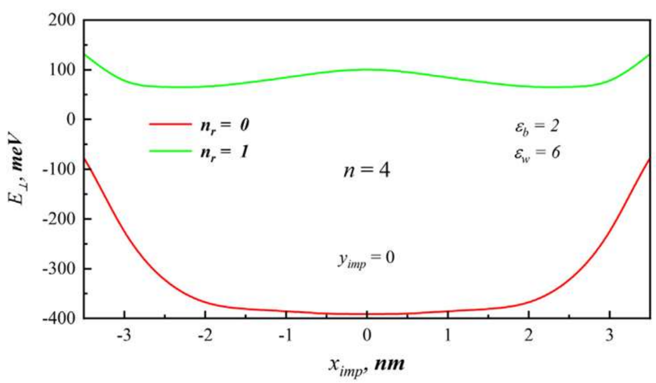

Fig. 5. Dependence of in-plane energy $E_\perp$ on the impurity position x_{imp} (for fixed y_{imp}) for the ground and first excited electron in-plane states with fixed $n = 4$, $\varepsilon_b = 2$.

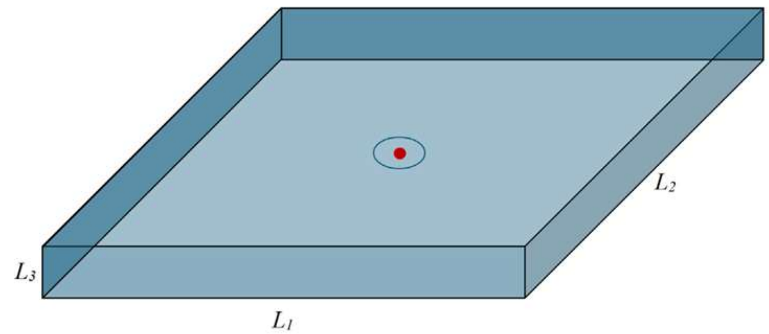

Fig. 2. Hydrogen-like impurity in $CdSe$ NPL.

$$\chi_{diam} = -\frac{e^2}{6\mu_\perp c^2}\int_{-\frac{L_1}{2}}^{\frac{L_1}{2}}\int_{-\frac{L_2}{2}}^{\frac{L_2}{2}} \psi^{*imp}_{\perp g.s.}\rho'^2\psi^{imp}_{\perp g.s.}\,dx\,dy$$

Publications (2025)

Nuclear Instruments and Methods in Physics Research A 1073 (2025) 170274

ELSEVIER

Contents lists available at ScienceDirect

Nuclear Inst. and Methods in Physics Research, A

journal homepage: www.elsevier.com/locate/nima

Full Length Article

Thermodynamic parameters of the electron gas in CdSe nanoplatelets

L.A. Tadevosyan [a], H.Ts. Ghaltaghchyan [b], V.A. Harutyunyan [b], Y.Sh. Mamasakhlisov [b,c,*], H.A. Sarkisyan [b]

$$Z_N = \frac{1}{N!}\left(\sum_{\{n\}} e^{-\beta E_{\{n\}}}\right)^N,$$

where $\beta = \frac{1}{k_B T}$, and N is the number of particles.

$$E_{\{n\}} = \frac{(\pi\hbar)^2}{2} \sum_{i=x,y,z} \frac{n_i^2}{\mu_i L_i^2},$$

where μ_i the effective mass

$$Z_0 = \sum_{n=1}^{\infty} e^{-\pi n^2 t}$$

A sum of the following form

$$\varphi(q) = \sum_{n=-\infty}^{\infty} q^{n^2}$$

is called Ramanujan's Theta function.

Publications (2025)

quantum reports

MDPI

Article

Thermodynamic and Magnetic Properties of Weakly Interacting Electron Gas Localized in a CdSe Cylindrical Core–Shell Quantum Dot

Levon Tadevosyan [1], Hayk Ghaltaghchyan [2], Yevgeni Mamasakhlisov [2,3] and Hayk Sarkisyan [2,*]

Abstract: The thermodynamic and magnetic properties of weakly interacting electron gas localized in a CdSe cylindrical core–shell quantum dot in the presence of axial magnetic field are investigated. The entropy, mean energy, and heat capacity of such a gas are determined, and its magnetic properties (magnetization and diamagnetic susceptibility) are studied. The possibilities of controlling thermodynamic parameters by changing the geometric parameters of quantum dots are shown. Calculations show that this gas has diamagnetic properties. These results provide insights into the features of physical processes occurring in thin core–shell quantum systems, which have potential applications in opto- and nanoelectronics.

Important paper

communications chemistry

PERSPECTIVE

Check for updates

https://doi.org/10.1038/s42004-021-00621-z OPEN

Curvature and self-assembly of semi-conducting nanoplatelets

Lilian Guillemeney[1], Laurent Lermusiaux[1], Guillaume Landaburu[1], Benoit Wagnon[1] & Benjamin Abécassis[1✉]

Semi-conducting nanoplatelets are two-dimensional nanoparticles whose thickness is in the nanometer range and controlled at the atomic level. They have come up as a new category of nanomaterial with promising optical properties due to the efficient confinement of the exciton in the thickness direction. In this perspective, we first describe the various conformations of these 2D nanoparticles which display a variety of bent and curved geometries and present experimental evidences linking their curvature to the ligand-induced surface stress. We then focus on the assembly of nanoplatelets into superlattices to harness the particularly efficient energy transfer between them, and discuss different approaches that allow for directional control and positioning in large scale assemblies. We emphasize on the fundamental aspects of the assembly at the colloidal scale in which ligand-induced forces and kinetic effects play a dominant role. Finally, we highlight the collective properties that can be studied when a fine control over the assembly of nanoplatelets is achieved.

Semiconductor nanoplatelets with curvature

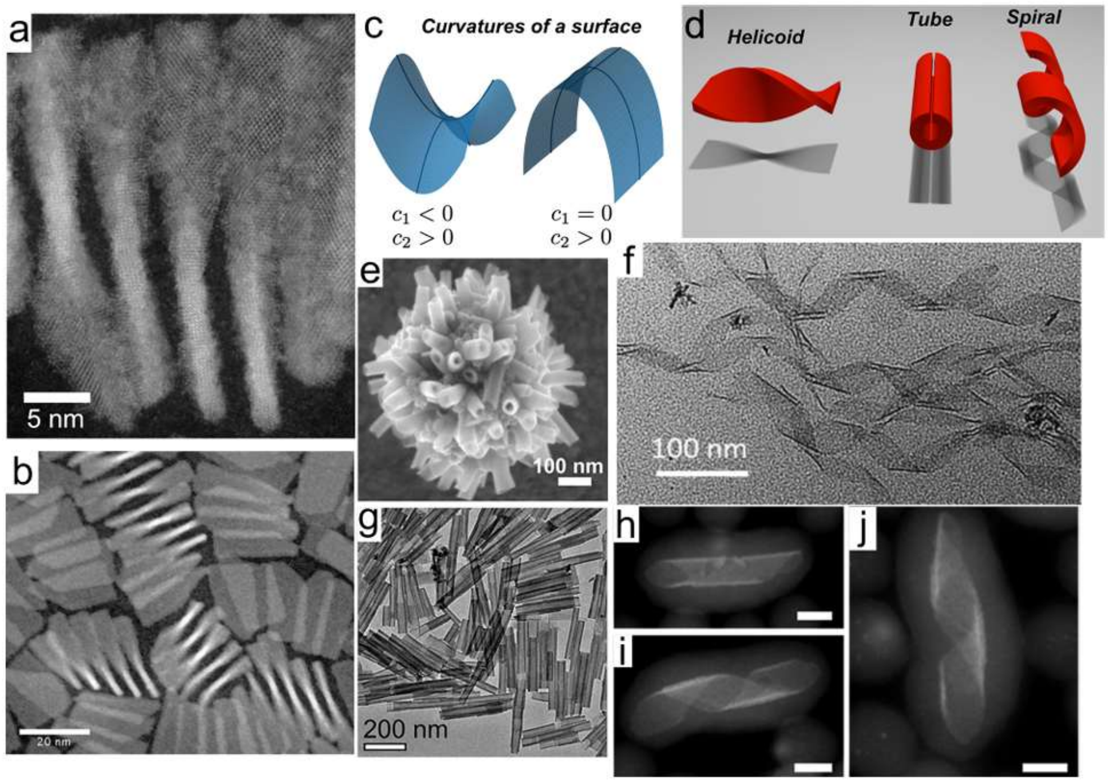

Fig. 2 Geometry of curved CdSe NPLs. a, **b** STEM images of 5 ML helicoidal NPL[46]. **c** Representation of the principal local curvatures of a surface. Left: the two principal curvatures have opposite signs leading to a negative Gaussian curvature $\kappa_2 = c_1 \times c_2$. Right: the Gaussian curvature is zero. **d** Different conformations of a ribbon. The shadows below the different shapes correspond to their projections on a surface and should thus resemble the TEM images of the corresponding particles. **e**, **g** CdSe 3 ML NPLs folded into tubular structures. Reprinted with permission from refs. [22,29]. Copyright 2019 and 2013 American Chemical Society. **f** 3 ML NPLs adopting a spiral ribbon geometry. Reprinted with permission from ref. [49]. Copyright 2019 American Chemical Society. **h**–**j** Spiral ribbons coated with a silica shell. Reprinted with permission from ref. [47]. Copyright 2014 American Chemical Society. Scale bars correspond to 5 nm.

Cylindrical core/shell quantum dot

174 (2023) 207471

Contents lists available at ScienceDirect

Micro and Nanostructures

journal homepage: www.journals.elsevier.com/micro-and-nanostructures

The electron gas in the core/shell cylindrical quantum dot: Thermodynamic and diamagnetic properties

H.Ts. Ghaltaghchyan [a], D.B. Hayrapetyan [a,b], E.M. Kazaryan [a,b], H.A. Sarkisyan [a,b,*]

[a] Russian-Armenian University, 123 Hovsep Emin, Yerevan, 0051, Armenia
[b] Peter the Great St.Petersburg Polytechnic University, 29 Polytechnicheskaya, St.Petersburg, 195251, Russia

ARTICLE INFO

Keywords:
cylindrical quantum dot
core/shell quantum dot
electron gas in quantum dot

ABSTRACT

Thermodynamic and magnetic properties have been investigated for the model of weak-interacting electron gas localized in the core/shell cylindrical quantum dot (QD) in the presence of an axial magnetic field. The radial analog of the two-dimensional potential of Winternitz-Smorodinsky has been considered as the radial confinement potential. It has been shown that gas has diamagnetic properties, wherein the magnetization practically has a linear dependence on the magnetic field. The system entropy, heat capacity and mean energy dependencies on magnetic field have been studied. In particular, it has been shown that with the increase of magnetic field, system entropy increases.

Cylindrical nanoplatelets

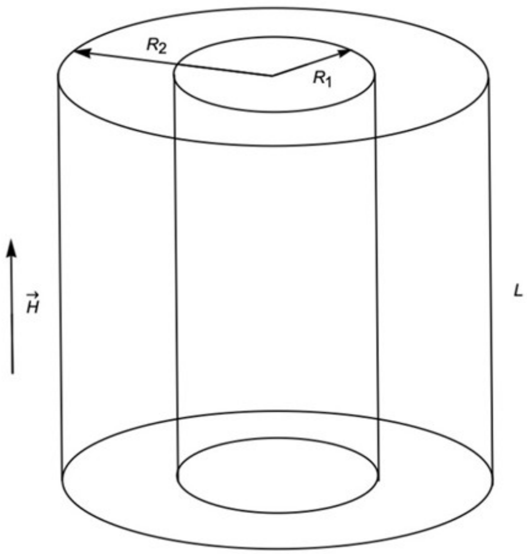

Figure 1. Schematic diagram of a thin core–shell cylindrical nanolayer.

$$V_{conf}(\rho, z) = V_{conf}{}^{(1)}(\rho) + V_{conf}{}^{(2)}(z),$$

$$V_{conf}{}^{(1)}(\rho) = \begin{cases} 0, R_1 \leq \rho \leq R_2 \\ \infty,\ \rho < R_1\ ,\ \rho > R_2 \end{cases}{}',$$

$$V_{conf}{}^{(1)}(z) = \begin{cases} 0, |z| \leq \frac{L}{2} \\ \infty, |z| > \frac{L}{2} \end{cases},$$

$$\frac{R_2 - R_1}{R_1} \ll 1$$

Flat rotator in a magnetic field

$$\hat{H} = \frac{1}{2\mu}\left(\overset{\rightarrow}{\hat{p}} - \frac{e}{c}\vec{A}\right)^2 + {V_{conf}}^{(1)}(\rho) + {V_{conf}}^{(2)}(z),$$

where $\overset{\rightarrow}{\boldsymbol{A}} = \left\{\boldsymbol{A}_\rho = \boldsymbol{A}_z = 0, \boldsymbol{A}_\varphi = \frac{B\rho}{2}\right\}$ and $\boldsymbol{\mu}$ is the effective mass of the electron.

$$\chi_{n_z}(z) = \sqrt{\frac{2}{L}}\sin\left(\frac{\pi n_z}{L}z + \delta_{n_z}\right), \qquad E_{n_z} = \frac{\pi^2\hbar^2{n_z}^2}{2\mu L^2},$$

where δ_{n_z} is the initial phase, for even states $\delta_{n_z} = \frac{\pi}{2}$, while for odd states, $\delta_{n_z} = 0$, n_z—axial quantum number. For the radial part of the Schrödinger equation, we will assume that the particle is at the ground level of radial quantization. Then, within the framework of the flat rotator model, we can assume that the electron rotates in a magnetic field with an effective radius $R_{eff} = \frac{R_1+R_2}{2}$. The corresponding Schrödinger equation for the angular part will have the following form:

$$\frac{\hbar^2}{2\mu{R_{eff}}^2}\frac{d^2\Phi}{d\varphi^2} + \frac{eB}{2\mu c}\frac{d\Phi}{d\varphi} + \frac{e^2B^2{R_{eff}}^2}{8\mu c^2}\Phi = E_{rot}\Phi,$$

Flat rotator in a magnetic field

Considering the symmetry of the problem, as well as the periodicity condition of the angular wave function $\Phi(\varphi + 2\pi) = \Phi(\varphi)$ for $\Phi(\varphi)$, we can write

$$\Phi(\varphi) = \Phi_m(\varphi) = \frac{1}{\sqrt{2\pi}} e^{im\varphi},$$

where $m = 0; \pm 1; \pm 2$ is the magnetic quantum number. Substituting expression (9) into the Schrödinger Equation (8) for the energy $E_{rot} \equiv E_m$, we obtain

$$E_m = \frac{\hbar^2}{2\mu {R_{eff}}^2} \left(m - \frac{\mathcal{F}}{\mathcal{F}_0} \right)^2,$$

where $\mathcal{F} = B\pi R^2$ is the magnetic field flux through a circle of radius R_{eff}, and $\mathcal{F}_0 = 2\pi \frac{\hbar c}{e}$ is the magnetic flux quantum. Thus, for the total energy of an electron, measured from the first level of radial quantization, we can write

$$E_{m,n_z} = \frac{\pi^2 \hbar^2 {n_z}^2}{2\mu L^2} + \frac{\hbar^2}{2\mu {R_{eff}}^2} \left(m - \frac{\mathcal{F}}{\mathcal{F}_0} \right)^2.$$

Partition function

$$Z_0 = \sum_{m=-\infty}^{+\infty} \sum_{n_z=1}^{\infty} e^{-\beta(E_m + E_{n_z})},$$

while $\beta = \frac{1}{KT}$.

$$S_1 = \sum_{n_z=1}^{\infty} e^{-\beta \frac{\pi^2 \hbar^2 {n_z}^2}{2\mu L^2}},$$

If we introduce the notation $\gamma_1 = \beta \frac{\pi \hbar^2}{2\mu L^2}$, then, taking into account the definition of Ramanujan's theta function $\varphi(q) = \sum_{n=-\infty}^{+\infty} q^{n^2}$, for S_1, we will have

$$S_1 = \sum_{n_z=1}^{\infty} e^{-\gamma_1 \pi {n_z}^2} = \frac{\varphi(e^{-\gamma_1 \pi}) - 1}{2},$$

$$q = e^{-\gamma_1 \pi}.$$

Partition function

$$S_2 = \sum_{m=-\infty}^{+\infty} e^{-\pi\gamma_2[m-\frac{\mathcal{F}}{\mathcal{F}_0}]^2},$$

where $\gamma_2 = \beta\frac{\hbar^2}{2\pi\mu R_{eff}{}^2}$. Let us note that for S_2, we can write the following:

$$S_2 = e^{-\pi\gamma_2(\frac{\mathcal{F}}{\mathcal{F}_0})^2} + \sum_{m=1}^{+\infty} e^{-\pi\gamma_2[m-\frac{\mathcal{F}}{\mathcal{F}_0}]^2} + \sum_{m=1}^{+\infty} e^{-\pi\gamma_2[m+\frac{\mathcal{F}}{\mathcal{F}_0}]^2},$$

$$m' \gg \frac{\mathcal{F}}{\mathcal{F}_0}, \qquad m - \frac{\mathcal{F}}{\mathcal{F}_0} \approx m,$$

$$Z = \frac{1}{N!}\{K^+(m') + K^-(m') - 2K(m') + \varphi(e^{-\gamma_2\pi}) - 1 + e^{-\pi\gamma_2(\frac{\mathcal{F}}{\mathcal{F}_0})^2}\}^N \times \left\{\frac{\varphi(e^{-\pi\gamma_1}) - 1}{2}\right\}^N.$$

Magnetic and thermodynamic parameters

Heat Capacity:

$$C_v = -\frac{1}{kT^2}\frac{\partial^2 Z(N)}{\partial (kT)^{-2}},$$

Entropy:

$$S = \frac{\partial}{\partial T}(kTlnZ(N)),$$

Magnetization:

$$M = \frac{kT}{Z(N)}\frac{\partial Z(N)}{\partial H},$$

Magnetic Susceptibility:

$$\chi = \frac{\partial \langle M \rangle}{\partial H},$$

Magnetic and thermodynamic parameters

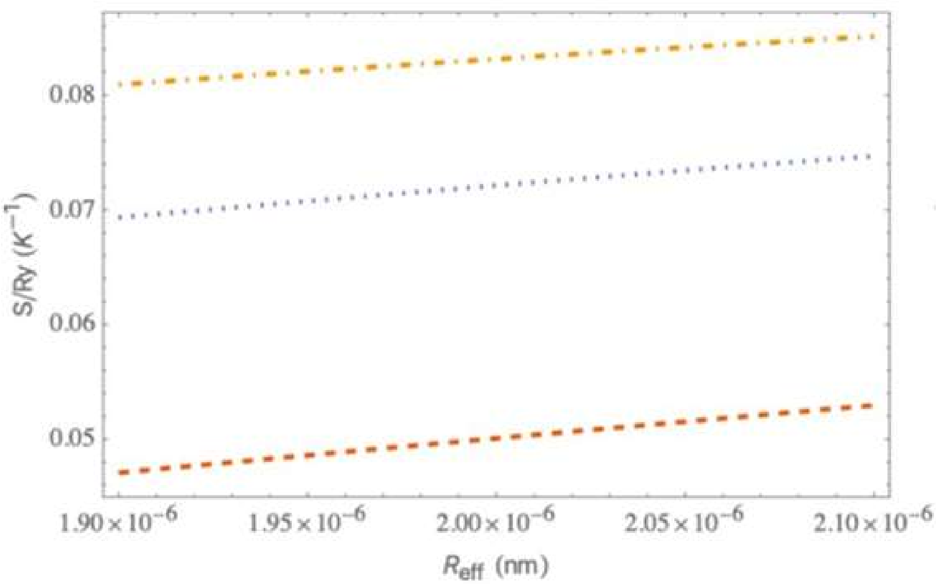

Figure 3. The dependency of the entropy of the electron gas on the R_{eff} at different temperatures, where Y-axis values are relative to the Rydberg energy and the values of X-axis values are in nanometers. Dashed red line corresponds to the temperature $T = 100$K, dotted blue line corresponds to $T = 200$K, and dot–dash orange line corresponds to $T = 300$K.

Magnetic and thermodynamic parameters

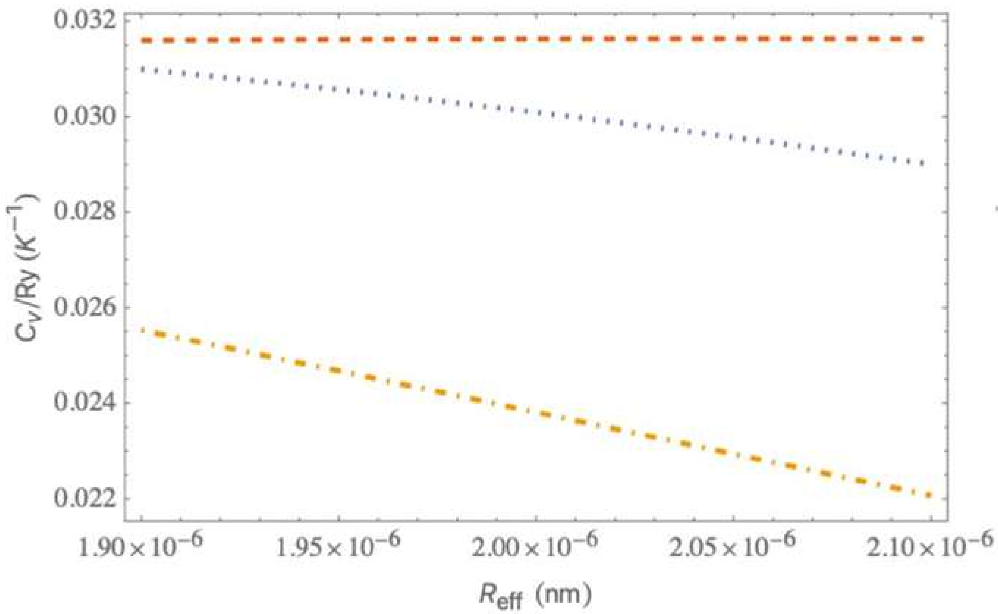

Figure 4. The dependency of the heat capacity of the electron gas on the R_{eff} at different temperatures, where Y-axis values are relative to the Rydberg energy and the values of X-axis values are in nanometers. Dashed red line corresponds to the temperature $T = 100$K, dotted blue line corresponds to $T = 200$K, and dot–dash orange line corresponds to $T = 300$K.

Magnetic and thermodynamic parameters

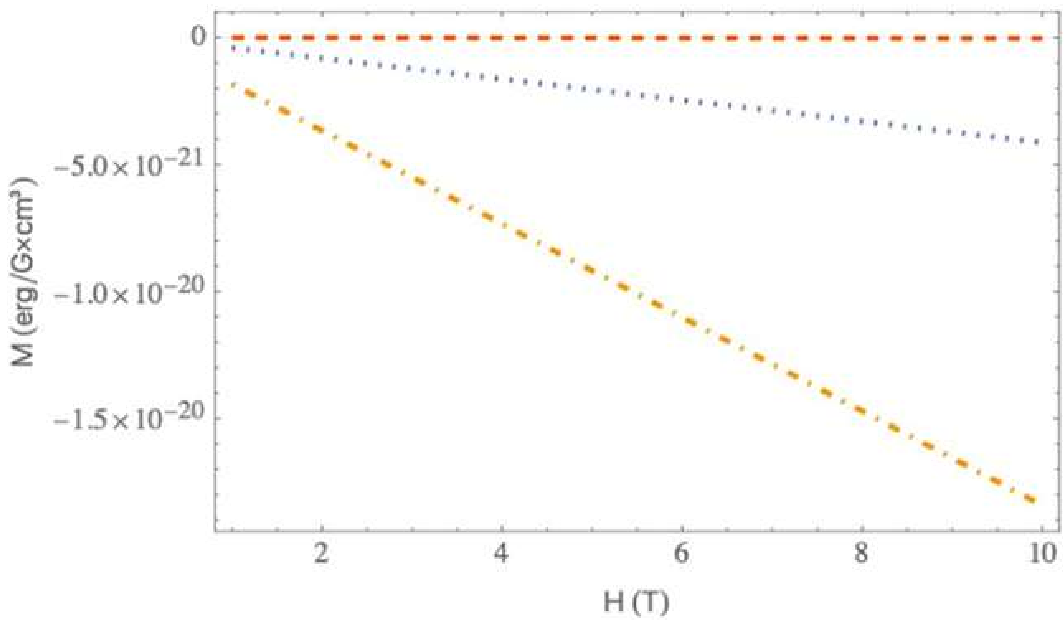

Figure 5. The dependency of the magnetization of the electron gas on the magnetic field at different temperatures, where the values of X-axis are in teslas. Dashed red line corresponds to the temperature $T = 100$K, dotted blue line corresponds to $T = 200$K, and dot–dash orange line corresponds to $T = 300$K.

Final remarks

- **Model of flat rotator is good approximation for modeling of one-particle states in CNPL**
- **With an increase in the effective radius of the CNPL, the entropy of the gas increases and the heat capacity decreasesImportant role of dielectric mismatch on the border of NP**
- **The electron gas localized in the CNPL has diamagnetic properties**

Thank you!